ORIGINAL ARTICLE

A C G publications

Rec. Nat. Prod. 11:1 (2017) 1-8

records of natural products

Bioactive Dammarane Triterpenoids from the Bark of *Drypetes acuminata* from Paluma, North Queensland, Australia

Suraj K. Pokharel[1], Mary Snow Setzer[1], Stefanie E. Greenleaf[1], Noura S. Dosoky[1], Betsy R. Jackes[2] and William N. Setzer[1*]

[1]*Department of Chemistry, University of Alabama in Huntsville, Huntsville, AL 35899, USA*

[2]*College of Science and Engineering, James Cook University, Townsville, Qld 4811, Australia*

(Received June 10, 2016; Revised September 05, 2016; Accepted September 07, 2016)

Abstract: Two known triterpenoids, friedelin and aglaitriol, and a new dammarane triterpenoid, aglaitriol 3-caffeate, have been isolated and identified in the chloroform bark extract of *Drypetes acuminata* P.I. Forst. (Putranjivaceae) from Paluma, north Queensland, Australia. The compounds were screened for antimicrobial and cytotoxic activity. Aglaitriol showed potent cytotoxic activity against three human tumor cell lines (MCF-7, MDA-MB-231, and 5637). Aglaitriol 3-caffeate showed moderate antibacterial activity against *Staphylococcus aureus* and *Escherichia coli*. A molecular docking analysis suggests topoisomerase II may be a likely protein target for aglaitriol.

Keywords: *Drypetes acuminata*; dammarane; aglaitriol; aglaitriol 3-caffeate; cytotoxicity; antibacterial; molecular docking.

1. Introduction

Drypetes acuminata P.I. Forst., previously known as *Drypetes lasiogyna* var. *australasica* (Müll. Arg.) Airy Shaw, is commonly known as yellow tulipwood or grey boxwood, although other names have been used [1]. The tree was formerly placed in Euphorbiaceae, but now is in the Putranjivaceae [2]. It is endemic to north east Queensland, Australia, where it is usually found in rainforest on granite substrate at altitudes between 600 and 1000 m. Members of the *Drypetes* genus are extensively used in African folk medicine to treat various diseases such as bronchitis, ailments of the digestive tract, fever, kidney pain and rheumatism [3,4] Members of this genus have shown anti-inflammatory, analgesic [5,6], antimicrobial [7-9], and cytotoxic [10,11] activities. Previous investigations of *D. acuminata* (syn. *D. lasiogyna*) from north Queensland, Australia, have shown the bark extracts to be antibacterial (*Staphylococcus aureus* and *Streptococcus pneumoniae*) and cytotoxic to human tumor cells (Hep-G2, MDA-MB-231, 5637) [12]. In this work, we present the isolation and characterization of biologically active dammarane triterpenoids from the chloroform bark extract of *D. acuminata*. To our knowledge, there have been no previous phytochemical studies of this tree.

2. Materials and Methods

2.1. General

NMR measurements (^{1}H, ^{13}C, HSQC, HMBC, COSY) were carried out on a Varian INOVA 500 MHz NMR spectrometer. IR measurements were obtained on a Perkin-Elmer Spectrum One FT-IR

* Corresponding author: E-Mail: setzerw@uah.edu

The article was published by Academy of Chemistry of Globe Publications
www.acgpubs.org/RNP © Published 21/09/2016 EISSN:1307-6167

spectrophotometer. HRMS/ESI were measured with a Bruker microOTO-Q II spectromer. Silica gel and TLC plates were obtained from Sorbtech Technologies (Norcross, Georgia, USA). HPLC grade chromatography solvents were obtained from Fisher Scientific (Waltham, Massachusetts, USA). Deuterochloroform was obtained from Sigma-Aldrich (St. Louis, Missouri, USA).

2.2. Plant Material

The bark of *D. acuminata* was collected on 31 July 1996 from the Paluma rainforest (Mt. Spec State Forest) of north Queensland, Australia (18º57′ S, 146º11′ E; elevation 900 m; 84 km north of Townsville) under permit issued to Dr. Betsy Jackes [12]. The plant was identified by Betsy Jackes and a voucher specimen is currently lodged at the James Cook Herbarium (JCT). The bark (1200 g) was chopped and extracted using a Soxhlet extractor and refluxing chloroform for 4 h. The chloroform was evaporated to give 68.6 g crude extract.

2.3. Chromatographic Separation

The crude bark extract (25.0 g) was subjected to bioactivity-directed column chromatography using silica gel (40-63 μm particle size and 60 Å porosity) as the stationary phase in a column of length 90 cm (length) × 5 cm (diameter). The elution was carried out using dichloromethane (DCM)/ethyl acetate (EtOAc) step gradient (Figure 1). The fractions (200-mL) were analyzed by thin-layer chromatography (TLC) and fractions with similar TLC profiles were combined.

Fractions F5-F7 (616.6 mg) were combined and purified by recrystallization from toluene to give 426.5 mg friedelin as a colorless crystalline solid. ^{1}H NMR ($CDCl_3$, 500 MHz), δ 2.39 (dd, 1H), 2.35-2.22 (m, 2H), 1.97 (m, 1H), 1.77 (m, 1H), 1.58 (m, 1H), 1.57-1.54 (m, 2H), 1.53-1.43 (m, 5H), 1.42-1.34 (m, 7H), 1.31-1.21 (m, 4H), 1.19 (s, 3H), 1.06 (s, 3H), 1.02 (s, 3H), 1.01 (s, 3H), 0.96 (s, 3H), 0.89 (d, 3H) 0.88 (s, 3H) 0.73 (s, 3H). ^{13}C NMR ($CDCl_3$, 125 MHz), δ 213.61, 77.16, 59.88, 58.63, 53.51, 43.20, 42.55, 41.94, 41.70, 40.10, 39.66, 38.70, 37.85, 36.42, 36.03, 35.75, 35.43, 33.18, 32.83, 32.50, 32.19, 30.91, 30.40, 28.58, 22.69, 20.67, 19.07, 18.64, 18.35, 15.07, 7.23. IR (KBr), 3380 (ν_{O-H}), 2929, 2868, 2351, 1713 ($\nu_{C=O}$), 1459, 1385, 1187, 1112, 784, 668 cm^{-1}.

Fractions F59-F65 (941.5 mg) were combined and subjected to column chromatography (silica gel, 24 cm L × 2 cm D, eluting with 95:5 DCM/MeOH step gradient, 20-mL fractions). Subfractions f15-f17 were combined and recrystallized from EtOAc/pentane to give 325.1 mg 5α-dammar-20-ene-3β,24,25-triol (aglaitriol) as a colorless crystalline solid. ^{1}H NMR ($CDCl_3$, 500 MHz), δ 4.78 (s, 1H), 4.73 (d, *J* = 1.35 Hz, 1H), 3.41 (d, *J* = 10.05 Hz, 1H), 3.19 (dd, *J* = 4.9, 11.55 Hz, 1H), 2.28-2.16 (m, 2H), 2.08-2.01 (m, 1H), 1.89 (s, 1H), 1.72-1.57 (m, 10H), 1.49-1.40 (m, 3H), 1.33-1.25 (m, 3H), 1.22 (s, 3H), 1.17 (s, 3H), 1.15-0.99 (m, 3H), 0.98 (s, 6H), 0.87 (s, 3H), 0.85 (s, 3H), 0.78 (s, 3H), 0.74 (dd, *J* = 2.15, 11.55, 1H). ^{13}C NMR ($CDCl_3$, 125 MHz), δ 15.79, 16.07, 16.34, 16.66, 18.70, 21.75, 23.67, 25.39, 26.97, 27.83, 28.43, 29.64, 30.50, 31.80, 31.95, 35.83, 37.63, 39.39, 39.51, 40.88, 46.05, 48.20, 49.88, 51.32, 56.28, 73.55, 77.16, 78.78, 79.36, 108.12, 153.26. IR (KBr), 3380 (ν_{O-H}), 2960, 2858, 1634 , 1447, 1413, 1385, 1360, 1299, 1245, 1083, 1048, 986, 941, 886, 783, 710 cm^{-1}. HRMS/ESI, m/z: obsd $[M+Na]^+$ 483.3821, calcd $[M+Na]^+$ 483.3814 for formula $C_{30}H_{52}O_3$.

Fractions F67-F69 (1.054 g) were combined and subjected to column chromatography (silica gel, 24 cm L × 2 cm D, eluting with 95:5 DCM/MeOH, 20-mL fractions). Subfractions f15-f17 were combined and recrystallized from EtOAc/pentane to give 141.7 mg dammar-20-ene-24,25-diol-3β-yl caffeate (aglaitriol 3-caffeate) as a colorless crystalline solid. ^{1}H NMR ($CDCl_3$, 500 MHz), δ 7.55 (d, *J* = 15.9 Hz, 1H), 7.09 (d, J = 1.9 Hz 1H), 7.00 (dd, J = 1.85, 8.30 Hz, 1H), 6.88 (d, J = 8.2 Hz, 1H), 6.28 (d J = 15.9 Hz, 1H), 4.79 (s, 1H), 4.73 (d, J = 1.05 Hz, 1H) 4.62 (dd, J = 5.57, 10.57 Hz, 1H), 3.41 (dd, J = 1.72, 10.47 Hz, 1H), 2.18- 2.29 (m., 1H), 1.99- 2.08 (m,1H), 1.91- 1.96 (m, 1H), 1.74 – 1.48 (m, 11H), 1.45 – 1.28 (m, 5H), 1.24 (s, 3H), 1.19 (s, 3H), 1.16 – 1.06 (m, 3H), 0.98 (s, 3H), 0.93 (s, 3H), 0.89 (s, 6H), 0.88 (s, 3H), 0.87 (m, 1H). ^{13}C NMR ($CDCl_3$, 125 MHz), δ 15.57, 15.83, 16.21, 16.59, 18.09, 21.27, 23.14, 23.74, 24.85, 26.45, 27.96, 29.11, 29.96, 31.30, 31.38, 35.25, 37.06, 38.06, 38.69, 40.40, 45.54, 47.69, 49.38, 50.72, 55.89, 73.19, 77.16, 78.33, 80.93, 107.68, 114.23, 115.36,

116.32, 122.23, 127.63, 143.70, 144.21, 146.03, 152.69, 167.33. HRMS/ESI, m/z: obsd $[M+Na]^+$ 645.4069, calcd $[M+Na]^+$ 645.4126 for formula $C_{39}H_{58}O_6$.

2.4. Antimicrobial Screening

The compounds were screened for antimicrobial activity against Gram-positive bacteria *Bacillus cereus* (ATCC No. 14579) and *Staphylococcus aureus* (ATCC No. 29213), and Gram-negative bacterium *Escherichia coli* (ATCC No. 10798). The minimum inhibitory concentrations (MIC) of the compounds against these microbes were determined by the microbroth dilution technique [12]. Solutions (50 μL of 1% w/v solutions of the samples in DMSO) were put into the top lane of 96 well plates and 50 μL of cation-adjusted Mueller Hinton broth (CAMHB) was added. The sample solutions were then serially diluted (1:1) by transferring 50 μL of sample CAMHB mixture to the next lane and adding 50 μL fresh CAMHB to obtain concentration from 2500 μg/mL to 12.5 μg/mL. The microbes were added to each well at a concentration of approximately 1.5×10^8 colony forming units (CFU)/mL. The plates were incubated at 37ºC for 24 hours and the final MIC was determined as the lowest concentration without any turbidity. Gentamicin was used as positive antimicrobial control and DMSO was used as negative control. Antifungal activity of the samples against *Candida albicans* (ATCC No. 90028) was determined as described above, in yeast-nitrogen base growth medium with final concentration of approximately 7.5×10^7 CFU/mL. Antifungal activity against *Aspergillus niger* (ATCC No. 16888) was determined similarly using potato dextrose broth inoculated with *A. niger* hyphal culture diluted to a McFarland turbidity of 1. Amphotericin B was used as positive control and DMSO was used as negative control for antifungal screening.

2.5. Cytotoxicity Screening

The compounds were screened for cytotoxic activity against MCF-7 human breast adenocarcinoma cells (ATCC No. HTB-22), MDA-MB-231 human breast adenocarcinoma cells (ATCC No. HTB-26), and 5637 human urinary bladder carcinoma cells (ATCC No. HTB-9) using a 96-well-based cytotoxicity assay [12]. MCF-7 and MDA-MB-231 cells were grown in RPMI 1640 supplemented with 10% Fetal bovine serum (FBS), 30mM HEPES, $NaHCO_3$, and penicillin-streptomycin. The 5637 cells were grown in RPMI 1640 supplemented with 10% FBS, 1mM sodium pyruvate, 2.5 g/L glucose, 30mM HEPES, $NaHCO_3$, and penicillin-streptomycin. Cells were plated into 96-well cell culture plates at concentration of 2.5×10^4 cells/well. The volume in each well was 100 μL. After 48 hours, supernatant fluid was removed by suction and replaced with 100 μL growth medium containing 1.0 μL of DMSO solution of the sample (1% w/w in DMSO), giving a final concentration of 100 μg/mL for each well. Solutions were added to wells in four replicates. Medium controls and DMSO controls (10 μL DMSO/mL) were used. Tingenone was used as a positive control [13]. In order to establish percent kill rates, the MTT assay for cell viability was carried out [14]. After colorimetric readings were recorded using SpectraMAX Plus microplate reader, at 570 nm, percent kill was calculated.

2.6. Molecular Docking

Protein-ligand docking was carried out using Molegro Virtual Docker [15,16] based on the crystal structures of farnesyl protein transferase (PDB 1JCQ [17]), topoisomerase II (PDB 1QZR [18] and PDB 2RGR [19]), DNA polymerase β (PDB 2BPC [20] and PDB 3UXN [21]), and 5-lipoxygenase (PDB 3V99 [22]). Prior to docking all solvent molecules and the co-crystallized ligands were removed from the protein structures. The ligand structures were built using Spartan ‘14 for Windows [23]. For each ligand, a conformational search and geometry optimization was carried out using the MMFF force field [24]. Molecular docking calculations for each protein were carried out with a sphere large enough to accommodate the substrate binding cavity (15 Å radius) to allow each ligand to search for possible docking conformations. Standard protonation states based on neutral pH were used throughout. Charges were assigned on each protein based on templates included in the

library files of Molegro Virtual Docker. Flexible ligand models were used in the docking and subsequent optimization. Variable orientations of each ligand were searched and ranked based on their re-rank score. For each docking simulation the maximum number of iterations for the docking algorithm was set to 1500, with a maximum population size of 50, and 30 runs per ligand. The RMSD threshold for multiple poses was set to 1.00 Å. The generated poses from each ligand were sorted by the calculated re-rank score.

3. Results and Discussion

Bioactivity-directed chromatographic separation of the crude chloroform bark extract of *Drypetes acuminata* (Figure 1) led to the isolation of friedelin (1.71% yield), aglaitriol (5α-dammar-20-ene-3β,24,25-triol) (1.30% yield), and aglaitriol 3-caffeate (dammar-20-ene-24,25-diol-3β-yl caffeate) (0.57% yield) (Figure 2). The structure of friedelin was readily determined by comparison of its ^{1}H and ^{13}C NMR and IR spectra with those reported in the literature [25-27]. The structure of aglaitriol was also confirmed by comparison of NMR and IR spectra with those previously reported [28]. The structure of aglaitriol 3-caffeate, reported for the first time, was elucidated by comparison of its ^{1}H and ^{13}C NMR spectra with agalitriol [28] and caffeic acid [29] (Table 1). Both ^{1}H and ^{13}C chemical shifts for aglaitriol and aglaitriol 3-caffeate were virtually identical. Comparison of the remaining NMR data with the NMR data for caffeic acid confirmed the identification of the caffeate ester. HMBC (Fig. 2) and COSY correlations confirmed the connectivity in the aglaitriol skeleton, and HMBC correlation between H-C(3) and C(1′)=O confirmed the location of the ester linkage. There are two possible epimers of aglaitriol and aglaitriol caffeate, (24*R*) and (24*S*). We were not able to discern which epimer was isolated in *D. acuminata*, however.

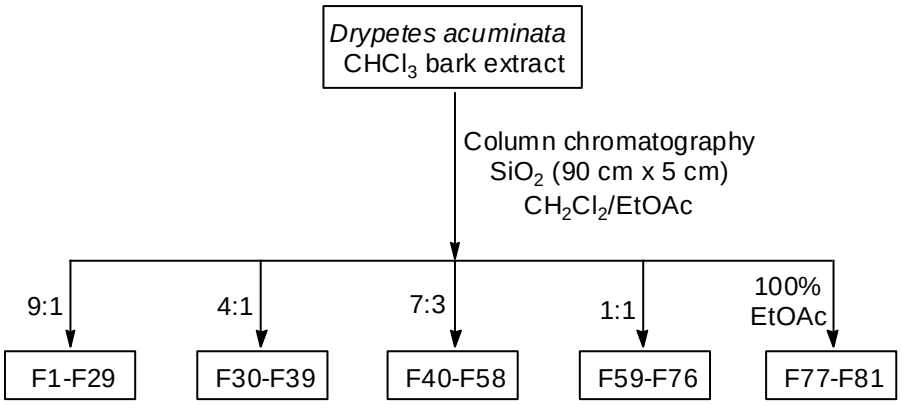

Figure 1. Preparative chromatographic separation scheme for *Drypetes acuminata* bark extract.

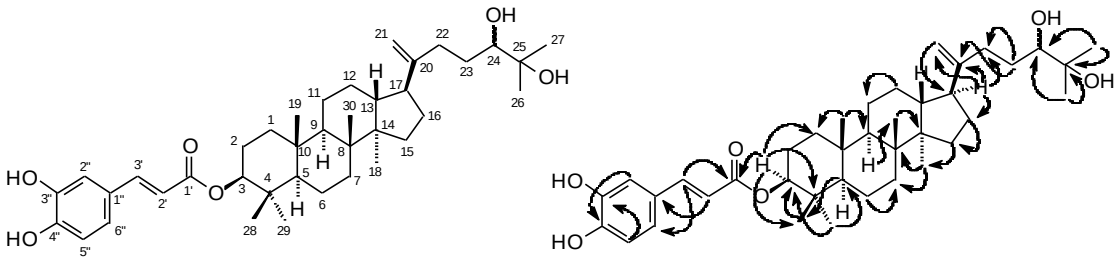

Figure 2. Numbering scheme (left) and key HMBC correlations (right) in aglaitriol 3-caffeate.

Antimicrobial screening revealed that only aglaitriol 3-caffeate had antibacterial activity against *S. aureus* and *E. coli* (MIC = 313 μg/mL, Table 2). None of the triterpenoids showed antifungal activity.

Table 1. ^{1}H and ^{13}C NMR data for aglaitriol and aglaitriol 3-caffeate (in $CDCl_3$, δ in ppm).

Position	Aglaitriol		Aglaitriol 3-caffeate	
	δ ^{13}C	**δ ^{1}H**	**δ ^{13}C**	**δ ^{1}H**
1	39.51	1.00, 1.71	38.69	1.07, 1.72
2	27.83	1.57, 1.62	23.74	1.57, 1.62
3	79.36	3.19 (dd)	80.93	4.62 (dd)[b]
4	39.39	---	38.06	---
5	56.28	0.74 (dd)	55.89	0.87
6	18.70	1.45, 1.55	18.09	1.45, 1.55
7	35.83	1.28, 1.58	35.25	1.28, 1.59
8	40.88	---	40.40	---
9	51.32	1.32	50.72	1.32
10	37.63	---	37.06	---
11	21.75	1.30, 1.57	21.27	1.34, 1.51
12	25.39	1.08, 1.57	24.85	1.08, 1.57
13	46.05	1.68	45.54	1.67
14	49.88	---	49.38	---
15	31.80	1.11, 1.62	31.30	1.11, 1.61
16	29.64	1.41, 1.92	29.11	1.41, 1.92
17	47.69	2.20	47.69	2.20
18	16.07	0.98 (s)	15.83	0.98 (s)
19	16.66	0.85 (s)	16.21	0.89 (s)
20	153.26	---	152.69	---
21	108.12	4.73 (d), 4.78 (s)	107.68	4.73 (d), 4.79 (s)
22	31.95	2.05, 2.28	31.38	2.05, 2.26
23	30.50	1.48, 1.68	29.96	1.48, 1.66
24	78.78	3.41 (d)	78.33	3.41 (d)
25	73.55	---	73.19	---
26	26.97	1.22 (s)	26.45	1.24 (s)
27	23.67	1.17 (s)	23.14	1.19 (s)
28	28.43	0.98 (s)	27.96	0.89 (s)
29	15.79	0.78 (s)	16.59	0.93 (s)
30	16.34	0.87 (s)	15.57	0.88 (s)
1′	*171.63*[a]	---	167.33[b]	---
2′	*117.04*	*6.24 (d)*	116.32	6.28 (d)
3′	*147.57*	*7.55 (d)*	144.21	7.55 (d)
1″	*128.29*	---	127.63	---
2″	*115.68*	*7.07 (d)*	114.21	7.09 (d)
3″	*147.16*	---	143.70	---
4″	*149.83*	---	146.03	---
5″	*115.98*	*6.81 (d)*	115.36	6.88 (d)
6″	*123.38*	*6.96 (dd)*	122.23	7.00 (dd)

[a] Caffeic acid NMR data (acetone-d_6) from Jeong et al. [29].
[b] Location of caffeate ester confirmed by HMBC correlation between H-C(3) and C(1′)=O.

Table 2. Antimicrobial activity of *D. acuminata* $CHCl_3$ crude bark extract and isolated triterpenoids.

Material	Antimicrobial activity (MIC, μg/mL)				
	B. cereus	*S. aureus*	*E. coli*	*S. albicans*	*A. niger*
D. acuminata extract	156	39	624	nt	nt
Friedelin	625	1250	2500	2500	2500
Aglaitriol	2500	2500	2500	2500	2500
Aglaitriol caffeate	2500	313	313	1250	2500

nt = not tested.

The triterpenoids were screened for cytotoxic activity against three human tumor cell lines, MCF-7 human breast adenocarcinoma, MDA-MB-231 human breast adenocarcinoma, and 5637 human urinary bladder carcinoma (Table 3). Aglaitriol showed remarkable cytotoxic activity against all three tumor cell lines. Neither friedelin nor aglaitriol caffeate were active in these assays, however. The mechanisms of activity of cytotoxic triterpenoids have been investigated [30] and several biochemical targets have been implicated, including farnesyl protein transferase [31], DNA polymerase β [32], lipoxygenase [33], and topoisomerase II [34,35].

Table 3. Cytotoxic activity of *D. acuminata* $CHCl_3$ crude bark extract and isolated triterpenoids.

Material	Cytotoxicity (%kill±SD at 100 μg/mL)		
	MCF-7	MDA-MB-231	5637
D. acuminata extract	nt	100	100
Friedelin	11.62±6.11	0	25.50±11.45
Aglaitriol	89.65±11.92	97.77±4.09	100
Aglaitriol caffeate	0	0	0

nt = not tested.

A molecular docking analysis has been carried out in order to provide some insight into the possible mechanism of cytotoxic activity of aglaitriol. Both (24*R*) and (24*S*) epimers of aglaitriol were examined in the docking analysis. Ursolic acid, which is known to be an inhibitor of DNA polymerase β, lipoxygenase, and topoisomerase II [30], was included in the docking analysis for comparison (Table 4). Both epimers of aglaitriol docked to the protein targets better (more exothermic) than the virtual positive control, ursolic acid. The protein-ligand interaction with the most exothermic docking energy was the DNA binding site of topoisomerase II, suggesting that this may be an important target in the cytotoxic activity of aglaitriol.

Table 4. MolDock rerank docking scores for aglaitriol with protein targets.

Ligand	Farnesyl protein transferase	Topoisomerase II		DNA Polymerase β		5-Lipoxygenase
	1JCQ	1QZR	2RGR	2BPC	3UXN	3V99
		ATP site	DNA site			
24*R*-Aglaitriol	-87.5	-77.7	-194.6	-97.0	-89.9	-107.8
24*S*-Aglaitriol	-99.4	-73.4	-207.9	-88.5	-79.1	-107.3
Ursolic acid	-78.5	-57.7	-149.6	-73.4	-70.9	-79.8

Acknowledgments

This work was partially supported by a grant from the National Institutes of Health to W.N.S. (R15 AIOD39740-01). We are very grateful to the Queensland Forest Service for allowing access to the State Forest at Paluma. We are grateful to Christen Posey for help with chromatographic separations, Prof. Bernhard Vogler for technical assistance with NMR data collection, and Ek Raj

Thapaliya (Laboratory of Molecular Photonics, Department of Chemistry, University of Miami, Florida) for collection of HRMS data.

Supporting Information

Supporting information accompanies with this paper on http://www.acgpubs.org/RNP

References

[1] P.I. Forster (1997). A taxonomic revision of *Drypetes* Vahl (Euphorbiaceae) in Australia. *Austrobaileya* **4**, 477-494.

[2] G. Levin (2014). Putranjivaceae, In: Flowering Plants. Endicots, The Families and Genera of Vascular Plants, vol 11, *ed:* K. Kubitzki, Springer-Verlag, Berlin, pp. 273-276.

[3] A. Bouquet and L. Debray (1974). Plantes Medicinales de la Cote-d'Ivoire, vol 32, Orstom, Paris, pp. 82-87.

[4] G.H. Schmelzer and A. Gurib-Fakim (2008). Medicinal Plants, Khuys Publishers, Wageningen, Netherlands, pp. 233-236.

[5] B. Chungag-Anye Nkeh, D. Njamen, A.B. Dongmo, J. Wandji, T.B. Nguelefack, J.D. Wansi, A. Kamanyi, and Z.T. Fomum (2001). Anti-inflammatory and analgesic properties of the stem extract of *Drypetes molunduana* Pax and Hoffm. (Euphorbiaceae) in rats, *Pharmaceut. Pharmacolog. Lett.* **11**, 61-63.

[6] S.J. Sudharshan, A. Chinmaya, N.C. Valleesha, T.R. Kekuda, A.N. Rajeshwara, and M. Syed (2009). Central nervous system (CNS) depressant and analgesic activity of methanolic extract of *Drypetes roxburghii* Wall in experimental animal model, *Res. J. Pharm. Technol.* **2**, 854-857.

[7] S.S. Awanchiri, H. Trinh-Van-Dufat, J.C. Shirri, M.D.J. Dongfack, G.M. Nguenang, S. Boutefnouchet, Z.T. Fomum, E. Seguin, P. Verite, F. Tillequin, and J. Wandji (2009). Triterpenoids with antimicrobial activity from *Drypetes inaequalis*, *Phytochemistry* **70**, 419-423.

[8] A. Ata, D.S. Tan, W.L. Matochko, and J.K. Adesanwo (2011). Chemical constituents of *Drypetes gossweileri* and their enzyme inhibitory and anti-fungal activities, *Phytochem. Lett.* **4**, 34-37.

[9] N. Joseph, F.M. Kasali, D.N. Patrice, T.K. Turibio and M.S. Ali (2015). Antimicrobial of extract and compounds from the bark of *Drypetes afzelii* (Pax) Hutch, *J. Pharmacog. Phytochem.* **4**, 250-255.

[10] Y.Z. Ge, H. Zhang, H.C. Liu, L. Dong, J. Ding, and J.M. Yue (2014). Cytotoxic dinorditerpenoids from *Drypetes perreticulata*, *Phytochemistry* **100**, 120-125.

[11] D. Chen, X. Cheng, Y. Sun, and P. Liu (2014). A new friedelane triterpenoid possessing cytotoxicity from the leaves and stems of *Drypetes hainanensis*, *Chem. Nat. Comp.* **50**, 93-96.

[12] M.C. Setzer, W.N. Setzer, B.R. Jackes, G.A. Gentry, and D.M. Moriarity (2001). The medicinal value of tropical rainforest plants from Paluma, north Queensland, Australia, *Pharmaceut. Biol.* **39**, 67-78.

[13] W.N. Setzer, M.C. Setzer, A.L. Hopper, D.M. Moriarty, G.K. Lehrman, K.L. Niekamp, S.M. Morcomb, R.B. Bates, K.J. McClure, C.C. Stessman, and W.A. Haber (1998). The cytotoxic activity of a *Salacia* liana species from Monteverde, Costa Rica, is due to a high concentration of tingenone, *Planta Med.* **64**, 583-583.

[14] M. Ferrari, M.C. Fornasiero, and A.M. Isetta (1990). MTT colorimetric assay for testing macrophage cytotoxic activity in vitro, *J. Immunol. Meth.* **131**, 165-172.

[15] Molegro Virtual Docker v. 6.0.1 (2013). Molegro ApS, Aarhus, Denmark.

[16] R. Thomsen and M.H. Christensen (2006). MolDock: a new technique for high-accuracy molecular docking, *J. Med. Chem.* **49**, 3315-3321.

[17] S.B. Long, P.J. Hancock, A.M. Kral, H.W. Hellinga, and L.S. Beese (2001). The crystal structure of human protein farnesyltransferase reveals the basis for inhibition by CaaX tetrapeptides and their mimetics, *Proc. Natl. Acad. Sci. U.S.A.* **98**, 12948-12953.

[18] S. Classen, S. Olland, and J.M. Berger (2003). Structure of the topoisomerase II ATPase region and its mechanism of inhibition by the chemotherapeutic agent ICRF-187. *Proc. Natl. Acad. Sci. U.S.A.* **100**, 10629-10634.

[19] K.C. Dong and J.M. Berger (2007). Structural basis for gate-DNA recognition and bending by type IIA topoisomerases, *Nature* **450**, 1201-1205.

[20] M.R. Sawaya, H. Pelletier, A. Kumar, S.H. Wilson, and J. Kraut (1994). Crystal structure of rat DNA polymerase β: Evidence for a common polymerase mechanism, *Science* **264**, 1930-1935.

[21] C.L. Gridley, S. Rangarajan, S. Firbank, S. Dalal, J.B. Sweasy, and J. Jaeger (2013). Structural changes in the hydrophobic hinge region adversely affect the activity and fidelity of the I260Q mutator DNA polymerase β., *Biochemistry* **52**, 4422-4432.

[22] N.C. Gilbert, Z. Rui, D.B. Neau, M.T. Waight, S.G. Bartlett, W.E. Boeglin, A.R. Brash, and M.E. Newcomer (2012). Conversion of human 5-lipoxygenase to a 15-lipoxygenase by a point mutation to mimic phosphorylation at serine-663, *FASEB J.* **26**, 3222-3229.
[23] Spartan '14 for Windows v. 1.1.0 (2014). Wavefunction Inc., Irvine, California.
[24] T.A. Halgren (1996). Merck molecular force field. I. Basis, form, scope, parameterization, and performance of MMFF 94., *J. Comput. Chem.* **17**, 490-519.
[25] T. Akihisa, K. Yamamota, T. Tamura, Y. Kimura, T. Iida, T. Nambara, and F.C. Chang (1992). Triterpenoid ketones from *Lingnania chungii* McClure: Arborinone, friedelin and glutinone, *Chem. Pharm. Bull.* **40**, 789-791.
[26] V. Castola, A. Bighelli, S. Rezzi, G. Melloni, S. Gladiali, J.M. Desjobert, and J. Casanova (2002). Composition and chemical variability of the triterpene fraction of dichloromethane extracts of cork (*Quercus suber* L.) *Ind. Crops Prod.* **15**, 15-22.
[27] P. Ghosh, A. Mandal, M. Chakraborty, and A. Saha (2010). Triterpenoids from *Quercus suber* and their antimicrobial and phytotoxic activities, *J. Chem. Pharmaceut. Res.* **2**, 714-721.
[28] O. Yodsaoue, J. Sonprasit, C. Karalai, C. Ponglimanont, S. Tewtrakui, and S. Chantrapromma (2012). Diterpenoids and triterpenoids with potential anti-inflammatory activity from the leaves of *Aglaia odorata*, *Phytochemistry* **76**, 83-91.
[29] C.H. Jeong, H.R. Jeong, G.N. Choi, D.O. Kim, U. Lee, and H.J. Heo (2011). Neuroprotective and anti-oxidant effects of caffeic acid isolated from *Erigeron annuus* leaf. , *Chin. Med.* **6**, 25 doi:10.1186/1749-8546-6-25.
[30] W.N. Setzer and M.C. Setzer (2003). Plant-derived triterpenoids as potential antineoplastic agents, *Mini Rev. Med. Chem.* **3**, 540-556.
[31] S. Sturm, R.R. Gill, H.B. Chai, O.D. Ngassapa, T. Santisuk, V. Reutrakul, A. Howe, M. Moss, J.M. Besterman, S.L. Yang, J.E. Farthing, R.M. Tait, J.A. Lewis, M.J. O'Neill, N.R. Farnsworth, G.A. Cordell, J.M. Pezzuto, and A.D. Kinghorn (1996). Lupane derivatives from *Lophopetalum wallichii* with farnesyl protein transferase inhibitory activity, *J. Nat. Prod.* **59**, 658-663.
[32] V.S.P. Chaturvedula, B.N. Zhou, Z. Gao, S.J. Thomas, S.M. Hecht, and D.G.I. Kingston (2004). New lupine triterpenoids from *Solidago canadensis* that inhibit the lyase activity of DNA polymerase β. *Bioorg. Med. Chem.* **12**, 6271-6275.
[33] A. Simon, A. Najid, A.J. Chulia, C. Delage, and M. Rigaud (1992). Inhibition of lipoxygenase activity and HL60 leukemic cell proliferation by ursolic acid isolated from heather flowers (*Calluna vulgaris*). *Biochim, Biophys. Acta* **1125**, 68-72.
[34] D.M. Moriarity, J. Huang, C.A. Yancey, P. Zhang, W.N. Setzer, R.O. Lawton, R.B. Bates, and S. Caldera (1998). Lupeol is the cytotoxic principle in the leaf extract of *Dendropanax* cf. *querceti*, *Planta Med.* **64**, 370-372.
[35] S.I. Wada, A. Iida, and R. Tanaka (2001). Triterpene constituents from the stem bark of *Pinus luchuensis* and their DNA topoisomerase II inhibitory effect, *Planta Med.* **67**, 659-664.